Computational Materials Science 48 (2010) 672–676

Contents lists available at ScienceDirect

Computational Materials Science

journal homepage: www.elsevier.com/locate/commatsci

Ab initio molecular dynamics study of pressure-induced phase transformation in KCl

Murat Durandurdu *

Department of Physics, University of Texas at El Paso, El Paso, TX 79968, USA
Fizik Bölümü, Ahi Evran Üniversitesi, Kırşehir 40100, Turkey

ARTICLE INFO

Article history:
Received 20 July 2009
Received in revised form 31 January 2010
Accepted 24 February 2010
Available online 29 March 2010

Keywords:
Phase transformation
Ab initio
Molecular dynamics
Metastable phase

ABSTRACT

We carry out an *ab initio* constant pressure molecular dynamics technique to study the pressure-induced phase transition in KCl. A phase transformation from the rocksalt structure to the CsCl type structure is successfully observed through constant pressure simulation. The rocksalt-to-CsCl phase transformation of KCl is found to proceed via a rhombohedral intermediate state. This phase transition is also analyzed from the total energy calculations. Our transition parameters and bulk properties are comparable with available experimental and theoretical data. Furthermore, we study the behavior of KCl under uniaxial stress. The uniaxial stress causes first a symmetry change to a tetragonal state with space group *I4/mmm* and then structural failure.

1. Introduction

The pressure-induced phase transformations from the sixfold to eightfold coordinated structure in binary compounds are a fundamental topic in condensed matter physics. Of particular interest are rocksalt (RS) structured materials. With the application of pressure, the RS phase (B1) often transforms into a CsCl type phase (B2). This phase transformation has been studied extensively for decades and considerable information concerning this phase change has been obtained. Yet a clear atomic level picture of this phase transition could not be obtained in static high-pressure experiments. In the past few years, much effort has been devoted to determine the transition mechanism of the B1-to-B2 phase transformation because an understanding of its mechanism is very important for technological applications and controlling transition process. To date several mechanisms has been proposed for this simple phase transformation. The first mechanism is known as Buerger mechanism [1] and based on compression of the primitive cell of the B1 structure along its threefold axis and hence a gradual increase of the rhombohedral angle of the intermediate $R\bar{3}m$ state from 60° to 90°. The second one was proposed by Watanabe, Tokonami and Morimoto (WTM) [2] and based on shifts of adjacent (0 0 1) planes of B1 leading to an intermediate orthorhombic *Pmmn* symmetry. Based on group-theoretical grounds, Stokes and Hatch [3] proposed 12 pathways. Among 12 mechanisms, a $P2_1/m$ monoclinic intermediate has the lowest activation barrier than the others. The fourth one was introduced by Tolédano et al. [4]; it consists of two consecutive displacive mechanisms, coupled to tensile and shear strains. This mechanism gives rise to two intermediate orthorhombic structures B16 and B33.

The activation energies of the two mechanisms ($R\bar{3}m$ and *Pmmn*) were found to be very close [5]. However, among these four mechanisms, the monoclinic and Tolédano pathways were found to be a lower enthalpy barrier than $R\bar{3}m$ and *Pmmn* for some RS structured materials [6,7]. Stokes et al. studied both monoclinic and Tolédano pathway for NaCl and PbS and found that their enthalpy barrier is approximately equal [7].

On the other hand, constant pressure simulations based empirical potentials so far support the Buerger, WTM or multiple intermediate phases [8–10]. Ruff et al. [8] performed molecular dynamics (MD) simulations in some alkali halides and suggested the WTM model for those materials. Using two different constant pressure algorithms, Parrinello–Rahman and modified Anderson pressure control technique, Nga and Ong [9] observed the formation of the WTM and Buerger mechanism in the same material and showed that both have the same intralayer rearrangement of ions but slightly different transitional movement of planes. In recent MD simulations, the transformation mechanism was found to be based on multiple intermediate phases [10]; the transformation starts with a Buerger $R\bar{3}m$ deformation of the B1 structure that is followed by the Stokes $P2_1/m$ mechanism leading to an intermediate B33 phase, which then connects to the B2 phase by using the Tolédano *Pbcm* pathway. The transition pressures predicted in some of these studies were considerably larger than the experimental transition pressures. The overestimated transition pressures lead to some doubts about the transformation mechanisms observed in these MD simulations because different transition pressures might produce different transformation

* Address: Department of Physics, University of Texas at El Paso, El Paso, TX 79968, USA.
E-mail address: mdurandurdu@utep.edu

0927-0256/$ - see front matter © 2010 Elsevier B.V. All rights reserved.
doi:10.1016/j.commatsci.2010.02.038

mechanisms. Zhang and Chen [11] produced the B1-to-B2 phase transition in NaCl at a transition pressure of 30 GPa, close to the experimental value of 30 GPa, using an empirical potential and suggested that the B1-to-B2 phase transition takes place with the characters of both Buerger and WTM mechanisms. The authors also studied KCl and proposed four different pathways. Although the intermediate states are obviously different along the four pathways, the simulations indicate that the essence of phase transition is reflected by a Buerger mechanism [11].

Recently using a constant pressure *ab initio* simulations, we studied the behavior of CdO and CaO under pressure. The phase transformation follows the rhombohedral intermediate phase in CdO [12] while it proceeds via two intermediate monoclinic phases, in CaO. These two different observations under similar conditions (the same simulation technique, the size of the simulation box and loading condition) might suggest that the B1-to-B2 phase change depends on material.

In principle, *ab initio* techniques produce more accurate results and hence they are ideally suited to eliminate limitations or doubts observed in empirical potentials. Here we use, for the first time, a constant pressure *ab initio* MD technique to study the pressure-induced phase transition in KCl and predict that the transformation pathway is based upon a rhombohedral intermediate phase.

2. Computational methods

The density functional calculations in the present work were performed within the generalized gradient approximation GGA [13] using the first-principles code SIESTA [14]. Norm-conservative Pseudopotentials were constructed using Troullier–Martins schemes [15]. A split-valence double-ξ plus polarized basis set was employed. A uniform mesh with a plane wave cut-off of 150 Ry was used to represent the electron density, the local part of the pseudopotentials, and the Hartree and the exchange–correlation potential. The simulation cell consists of 64 atoms with periodic boundary conditions. We used Γ-point sampling for the Brillouin zone integration. The molecular dynamics (MD) simulations were performed using the NPH (constant number of atoms, constant pressure, and constant enthalpy) ensemble. The reason for choosing this ensemble is to remove the thermal fluctuation, which facilitates easier examination of the structure during the phase transformation. Pressure was applied via the method of Parrinello and Rahman [16]. At each applied pressure, the structure was equilibrated with a period of 1000 time steps (each time step is one femto-second (fs)). We also used the power quenching technique during the MD simulations. In this technique, each velocity component is quenched individually. At each time step, if the force and velocity components have opposite sign, the velocity component is set equal to zero. All atoms or supercell velocities (for cell shape optimizations) are then allowed to accelerate at the next time step. For the uniaxial stress simulations, a uniaxial stress was applied along the [0 0 1] direction, while the other stress components were initially set to zero, and the simulation cell lengths were allowed to adjust to the applied stress. For the energy–volume calculations, we used the primitive cell for both B1 and B2 phases and the Brillouin zone integration was performed with automatically generated $8 \times 8 \times 8$ k-point mesh for both phases following the convention of Monkhorst and Pack [17]. In order to determine the intermediate state during the phase transformation, we used the KPLOT program [18] that supplies detailed information about space group, cell parameters and atomic position of a given structure. For the symmetry analysis we used 0.2 Å, 2°, and 0.7 Å tolerances for bond lengths, bond angles and interplanar spacing, respectively.

3. Structural properties and enthalpy calculations

In order to validate the parameters used in the simulations, we first optimize the lattice constants of both B1 and B2 phases and summarize our results, with available experimental and the other theoretical data, in Table 1. Overall we find a reasonable agreement between our results and experimental and theoretical values [19–25].

In order to predict the transition pressure between B1 and B2 phases and calculate their bulk properties, we study their total energies as a function of volume and fit the energy–volume data to the third order Birch–Murnaghan equation of state. Fig. 1 shows the energy–volume relations. From the energy–volume data, we simply calculate pressure $P = -\mathrm{d}E_{\mathrm{tot}}/\mathrm{d}V$ (obtained by direct differentiation of the energy–volume curves) and the static enthalpy $H = E_{\mathrm{tot}} + PV$. Since at the phase transition the two phases have the same enthalpy, the transition pressure can be easily determined by equating the enthalpy of the two phases. The computed enthalpy curves are plotted as a function of pressure in Fig. 2. Our transition pressure for B1-to-B2 phase change transition occurs around 2.4 GPa, which is in good agreement with the experimental and theoretical results of about 2 GPa (see Table 2) [8,19,21–23,26,27].

We also obtain the bulk modulus, its pressure derivative and the transition parameters from the third order Birch–Murnaghan equations of state. The calculated values are also given in Tables 1 and 2. In general, our data agree with both experimental and theoretical results [8,19–27].

These data indicate that the parameters used in the simulations are good enough to produce reasonable results and hence they can be applied to study the pressure-induced phase transitions in the dynamical simulations.

4. B1-to-B2 phase transformation from the dynamical simulation

Fig. 3 shows the pressure dependence of volume. As seen from the figure, the volume decreases gradually and at 18 GPa, it abruptly declines, indicating a first order phase transformation at this pressure. The structural analysis using the KPLOT program reveals that the RS structure transforms into a CsCl structure. This finding indicates that the *ab initio* technique successfully generates the experiment observed high-pressure phase of KCl with an overestimated transition pressure, relative to the experimental transition pressure of about 2.0 GPa. Such an overestimation in transition pressures, in analogous to superheating MD simulations, is usually seen in constant pressure simulations and implies a high

Table 1
Lattice parameters, bulk modulus B_o, and its pressure derivative B'_o for B1 and B2 phases of KCl.

Phase	a (Å)	B_o (GPa)	B'_o	Reference
B1	6.271	20.94	5.9	This study
	6.32	18.6		[19] (Theory)
	6.294	15.5		[20] (Theory)
	6.2	19.3	5.16	[21] (Theory)
	6.32	17.2	3.89	[22] (Theory)
	6.53	15.5		[23] (Theory)
	6.57	15.7		[24] (Theory)
		17.43	5.23	[25] (Experiment)
	6.29	19.7	4.03	[19] (Experiment)
B2	3.734	24.36	5.7	This study
	3.79	20.07	3.41	[22] (Theory)
	3.76			[19] (Theory)
	3.71	26.8	4.82	[21] (Theory)
	3.38	19.6		[23] (Theory)

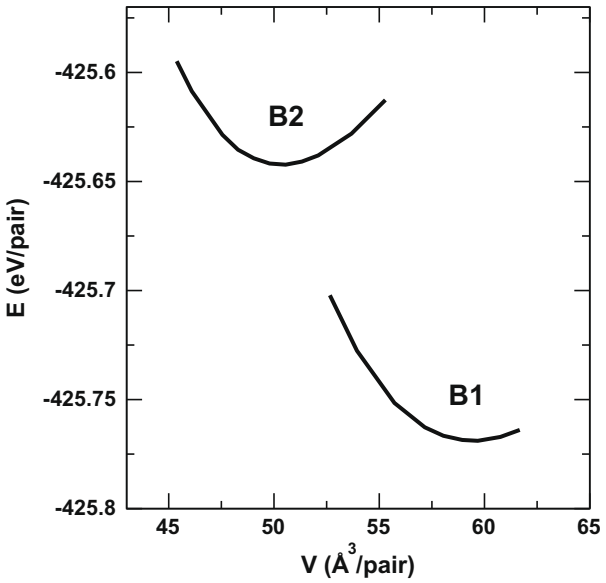

Fig. 1. Computed energies of B1 and B2 phases as a function of volume.

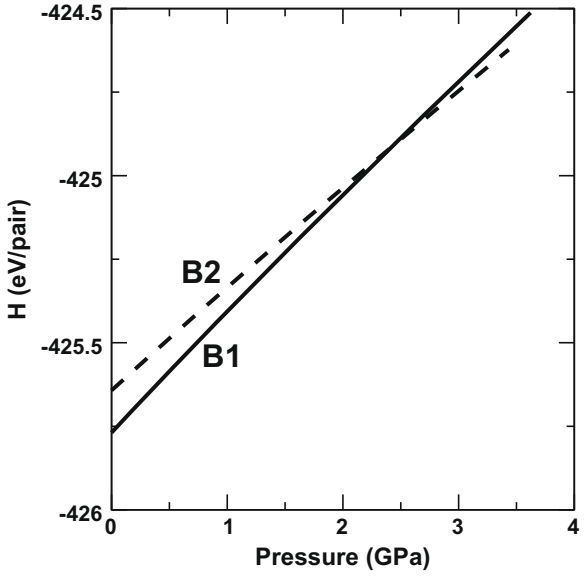

Fig. 2. Calculated enthalpy curve of B1 and B2 structures as a function of pressure.

intrinsic activation barrier for transforming one solid phase into another in simulations. When the particular conditions such as finite size of the simulation cell, the lack of any defect in simulated

Table 2
The transition parameters; critical pressure P_t, the transitions volumes V_t/V_0 (B1) and V_t/V_0 (B2), the volume change $-\Delta V_t/V_t$ during the phase transformation. Refs. [19,27] are experiment.

P_t	V_t/V_0 (B1)	V_t/V_0 (B2)	$-\Delta V_t/V_t$	Reference
2.4	0.91	0.79	0.13	This study
2.8	0.88	0.89	0.12	[22]
1.1	0.968	0.835	0.137	[26]
2.0	0.915	0.803	0.123	[27]
2.4	0.90	0.78	0.10	[19]
2.58	0.90	0.91	0.10	[8]
2.1			0.12	[21]
2.0			0.13	[23]

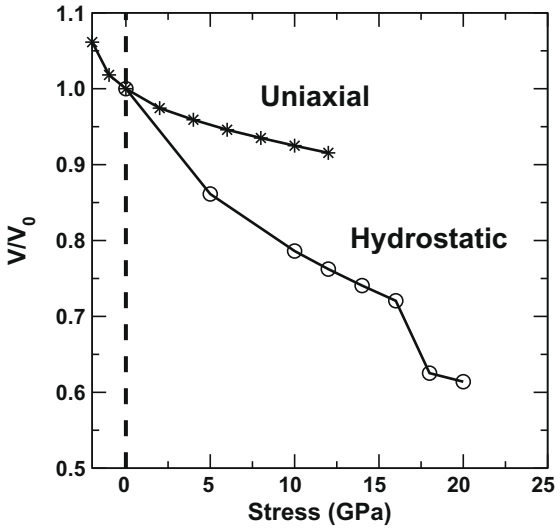

Fig. 3. Volume change as a function of hydrostatic pressure and uniaxial stress.

structure, the time scale of simulations and the absence of surfaces in simulated structures. are considered, such an overestimated transition pressure is anticipated. This activation barrier can overcome if the simulated structures are overpressurized. On the other hand, the thermodynamic theorem does not take into account the possible existence of such an activation barrier separating the two structural phases and hence the transition pressure obtained the

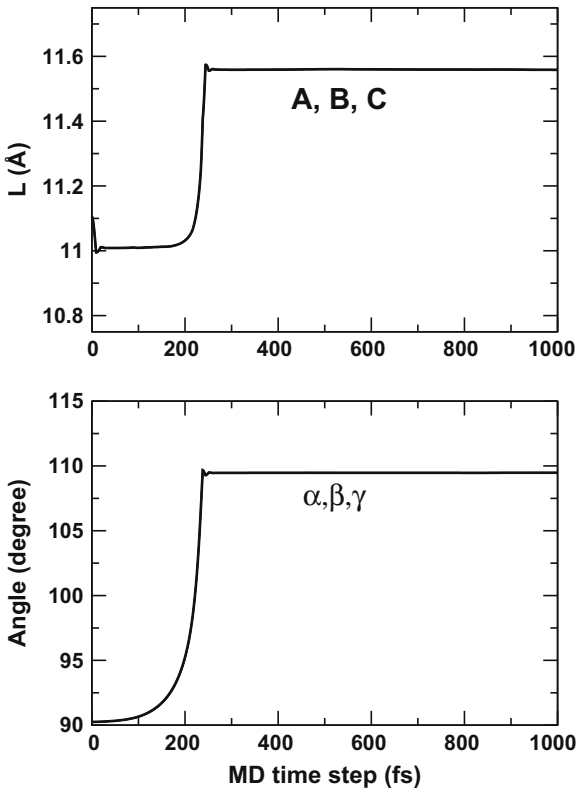

Fig. 4. The simulation cell lengths and angles as a function of MD time step at 18 GPa. The lattice vectors **A**, **B** and **C** are along the [0 0 1], [0 1 0] and [0 0 1] directions, respectively and their magnitude is plotted in the figure. During the phase transformation, the simulation cell lengths change with the same magnitude and hence they are overlap. The simulation cell angles α, β and γ are also modified by the same degree.

MD simulation differs from the one predicted using the thermodynamic theorem.

The modification of simulation cell during the phase change provides substantial information about the mechanism of this transformation at the atomistic level and hence as a next step we study the variation of the simulation cell lengths and angles as a function of MD time step and plot them in Fig. 4. The simulation box is initially a cubic cell whose lattice vectors are along the [0 0 1], [0 1 0] and [0 0 1] directions, respectively. The magnitude of these vectors is plotted in the figure. As clearly seen from the figure, the system undergoes dramatic reconstructions after around 100 fs. All simulation cell angles gradually changes from 90° to about 110° and the simulation cell lengths slightly increase. This mechanism is similar to what has been observed in the classical MD simulations in which two angles become about 70.4° while the third one is 110° [11]. These modifications are simply equivalent to the distortions observed in our simulations.

In order to characterize any intermediate state(s) formed during the B1-to-B2 phase transformation of KCl, we carefully analyze the structure at each MD step using the KPLOT program. At 200 fs, we determine a rhombohedral state whose lattice parameters are $a = b = c = 3.702$ Å and angles $\alpha = \beta = \gamma = 67.18°$. In later time steps, the lattice constants gradually decrease while the angles tend to increase to 90° at which point the CsCl type phase whose lattice constants $a = b = c = 3.33$ Å is formed around 252 fs.

5. Uniaxial stress

In addition to hydrostatic pressure, studies of the structural and mechanical responses of materials at finite strain are crucial for our understanding of many areas such as phase transformation, theoretical strength, crack propagation and nanotechnology. We are not aware of any study that explores the behavior of KCl under a uniaxial stress. The lack of such information stimulates us to investigate systematically the stability of KCl subjected to a uniaxial stress. We apply both tensile and compressive stresses along [0 0 1] direction. The volume change as a function of uniaxial stress is also given in Fig. 3. As seen from the figure, the volume decreases with increasing compressive uniaxial stress (in the tensile regime, the volume increases) but the change in the volume is quite less than that of hydrostatic case as expected. KCl exhibits structural failure at −3 GPa and 14 GPa in our simulation. Certainly, these critical stresses are overestimated in the simulation as in the hydrostatic case. We cannot however absolutely tell the degree of the overestimation of these critical stresses in the simulation because we are not aware of any experimental studies on the behavior of KCl under uniaxial stresses but we suppose that they are a factor of 8–9 times larger than the experimental values as in the hydrostatic compression and hence we expect to see the structural failure of KCl around −0.25 GPa and 1.5 GPa in experiments.

The stress dependence of the simulation cell lengths is depicted in Fig. 5. The axis compressed decreases gradually while the others tend to increase because the structure attempts to converse its volume. In the tensile regime, we observe the opposite tendency; the axis tensioned increases while the others decrease. The simultaneous construction and expansions of the cell lengths change the structure from cubic to tetragonal without causing any coordination modification. The tetragonal structure has *I4/mmm* symmetry.

A uniaxial compression of a solid usually yields an expansion in the transfer directions. This behavior is described by the Poisson ratio that is used to characterize a material's elastic properties. The Poisson ratio of a solid subjected to a uniaxial stress is defined as the negative ratio of transfer strain in the i direction resulting from an applied strain in the j direction. The Poisson ratio for a cubic simulation box compressed uniaxially along the [0 0 1]-axis is given by

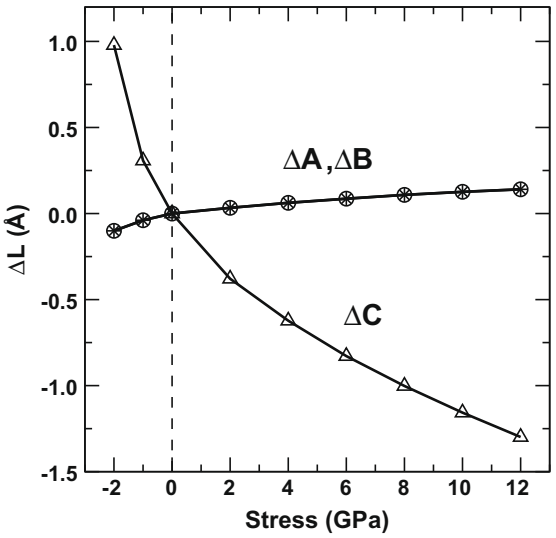

Fig. 5. Change of the simulation cell lengths ($\Delta L = L_{\text{stress}} - L_{\text{zero-stress}}$, where $L = |\mathbf{A}|$, $|\mathbf{B}|$ and $|\mathbf{C}|$) as a function of applied uniaxial stress. The zero-stress value of $|\mathbf{A}|$, $|\mathbf{B}|$ and $|\mathbf{C}|$ is 12.54 Å. The lattice vectors **A**, **B** and **C** are along the [0 0 1], [0 1 0] and [0 0 1] directions, respectively.

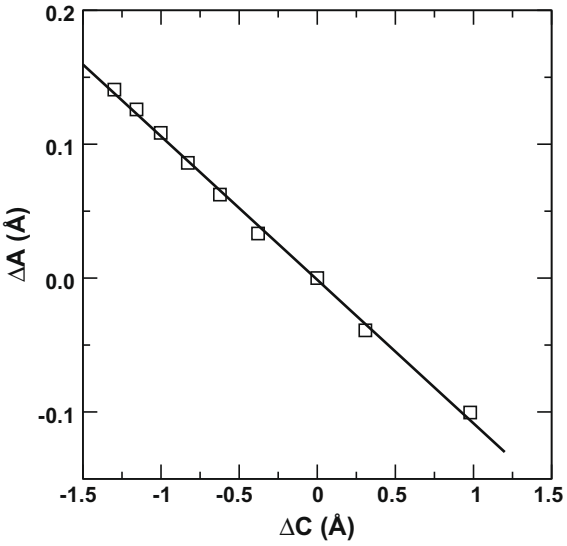

Fig. 6. Variation of ΔA as a function of ΔC.

$$\sigma_{xz} = -\frac{\Delta A}{\Delta C}$$

The variation of ΔA and ΔC in the pressure range from −2 GPa to 12 GPa is illustrated in Fig. 6. The slope of the best fitting straight line gives 0.11 for the Poisson ratio of KCl at zero pressure, which is in good agreement with the value of 0.14 [28].

6. Discussion

We have studied the behavior of several B1 structured materials using constant pressure *ab initio* simulations and observed the rhombohedral intermediate state for CdO and KCl and monoclinic intermediate states for CaO. The observation of different transformation mechanisms in these systems using the same simulation technique, the size of the simulation box and loading condition might state that the B1-to-B2 phase transformation might be material dependent. Based on only two different observations we

cannot however explain which properties of the B1 structured materials drive a specific transformation mechanism. Therefore, further studies are certainly needed to explain the physical origin of distinct transformation mechanisms observed for the B1-to-B2 phase transformations.

7. Conclusions

We have used an *ab initio* constant pressure technique to study the pressure-induced phase transition in the KCl and observed a phase change from the B1-to-B2. Furthermore, we describe the transformation mechanism and show that it proceeds by a rhombohedral intermediate state, validating previous MD simulations based on empirical potentials. This phase transformation is also analyzed using the energy–volume calculations. The computed transition parameters and bulk properties are in good agreement with experimental and theoretical data. Furthermore we study the response of KCl to the uniaxial stresses (tensile and compressive) and find no indication a new phase transformation but structural failure.

Acknowledgements

The visit of the author to Ahi Evran Üniversitesi was facilitated by the Scientific and Technical Research Council of Turkey (TÜBİTAK) BIDEB-2221. The calculations were run on Sacagawea, a 128 processor Beowulf cluster, at the University of Texas at El Paso.

References

[1] M. Buerger, in: R. Smoluchowski, J.E. Mayers, W.A. Weyl (Eds.), Phase Transformations in Solids, Wiley, New York, 1948, pp. 183–211.
[2] M. Watanabe, M. Tokonami, N. Morimoto, Acta Crystallogr., Sect. A: Cryst. Phys., Diffr., Theor. Gen. Crystallogr. A 33 (1977) 284.
[3] H.T. Stokes, D.M. Hatch, Phys. Rev. B 65 (2002) 144114.
[4] P. Tolédano, K. Knorr, L. Ehm, W. Depmeier, Phys. Rev. B 67 (2003) 144106.
[5] C.E. Sims, G.D. Barrera, N.L. Allan, W.C. Mackrodt, Phys. Rev. B 57 (1998) 11164.
[6] M. Catti, Phys. Rev. B 68 (2003) 100101.
[7] H.T. Stokes, D.M. Hatch, J. Dong, J.P. Lewis, Phys. Rev. B 69 (2004) 174111.
[8] I. Ruff, A. Baranyi, E. Spohr, K. Heinzinger, J. Chem. Phys. 91 (1989) 3149.
[9] Y.A. Nga, C.K. Ong, Phys. Rev. B 46 (1992) 10547.
[10] R.C. Mota, P.S. Branício, J.P. Rino, Europhys. Lett. 76 (2006) 836.
[11] S. Zhang, N.-X. Chen, Modell. Simulat. Mater. Sci. Eng. 11 (2003) 331; S. Zhang, N.-X. Chen, Acta Mater. 51 (2003) 6151.
[12] M. Durandurdu, Europhys. Lett. 84 (2008) 66003.
[13] J.P. Perdew, K. Burke, M. Ernzerhof, Phys. Rev. Lett. 77 (1996) 3865.
[14] P. Ordejón, E. Artacho, J.M. Soler, Phys. Rev. B 53 (1996) 10441; D. Sánchez-Portal, P. Ordejón, E. Artacho, J.M. Soler, Int. J. Quantum Chem. 65 (1997) 453.
[15] N. Troullier, J.L. Martins, Phys. Rev. B 43 (1997) 1993.
[16] M. Parrinello, A. Rahman, Phys. Rev. Lett. 45 (1980) 1196.
[17] H.J. Monkhorst, J.D. Pack, Phys. Rev. B 13 (1976) 5188.
[18] R. Hundt, J.C. Schön, A. Hannemann, M. Jansen, J. Appl. Crystallogr. 32 (1999) 413.
[19] A.J. Cohen, R.G. Gordon, Phys. Rev. B 12 (1975) 3228.
[20] A.M. Pendás, V. Luaña, J.M. Recio, M. Flórez, E. Francisco, M.A. Blanco, L.N. Kantorovich, Phys. Rev. B 49 (1994) 3066.
[21] H. Zhang, M.S.T. Bukowinski, Phys. Rev. B 44 (1991) 2495.
[22] Z.J. Chen, H.Y. Xiao, X.T. Zu, Chem. Phys. 330 (2006) 1.
[23] A.M. Pendas, V. Luana, Phys. Rev. B 49 (1994) 3066.
[24] M. Prencipe, A. Zupan, R. Dovesi, Phys. Rev. B 51 (1995) 3391.
[25] E.A. Perez-Albuerne, H.G. Drickamer, J. Chem. Phys. 43 (1965) 1381.
[26] S. Froyen, M.L. Cohen, J. Phys. C: Solid State Phys. 19 (1986) 2623.
[27] S.N. Vaidya, G.C. Kennedy, J. Phys. Chem. Solids 32 (1971) 551.
[28] A.N. Norris, Proc. Roy. Soc. A 462 (2006) 3385.